COMMUNICATIONS IN COMPUTATIONAL PHYSICS
Vol. **5**, No. 2-4, pp. 376-390

Commun. Comput. Phys.
February 2009

Development of Residual Distribution Schemes for the Discontinuous Galerkin Method: The Scalar Case with Linear Elements

Rémi Abgrall[1,*] and Chi-Wang Shu[2]

[1] *Institut de Mathématiques and INRIA, Université Bordeaux I, 341 cours de la Libération, 33 405 Talence cedex, France.*
[2] *Division of Applied Mathematics, Brown University, Providence, RI 02912, USA.*

Received 30 September 2007; Accepted (in revised version) 31 March 2008

Available online 1 August 2008

Abstract. In this paper, we reformulate the piecewise linear discontinuous Galerkin (DG) method for solving two dimensional steady state scalar conservation laws in the framework of residual distribution (RD) schemes. This allows us to propose a new class of nonlinear stabilization that does not destroy the formal accuracy of the schemes. Numerical results are shown to demonstrate the behavior of this approach.

AMS subject classifications: 65N30, 65N99, 65M60, 65M99

Key words: Discontinuous Galerkin schemes, residual distribution schemes, high order, unstructured meshes.

1 Introduction

We consider the scalar Cauchy problem

$$\begin{array}{ll} \dfrac{\partial u}{\partial t}+\operatorname{div}\mathbf{f}(u)=0, & x\in\Omega, \\ u(x,t=0)=u_0, & x\in\Omega, \\ u(x,t)=g(x,t), & x\in\partial\Omega^-,\ t>0, \end{array} \tag{1.1}$$

and its steady version,

$$\begin{array}{ll} \operatorname{div}\mathbf{f}(u)=0, & x\in\Omega, \\ u(x)=g(x), & x\in\partial\Omega^-. \end{array} \tag{1.2}$$

Here Ω is the computational domain and $\partial\Omega^-$ is the inflow part of the domain boundary.

*Corresponding author. *Email addresses:* abgrall@math.u-bordeaux.fr (R. Abgrall), shu@dam.brown.edu (C.-W. Shu)

A very popular class of numerical methods to approximate (1.1) is the discontinuous Galerkin (DG) method [1]. It uses a finite element representation of the solution within each element of a triangulation of Ω, and the approximation function is discontinuous across the edges (or faces in 3D) of the mesh elements. The second ingredient is a weak formulation of (1.1) combined with a flux formulation for the element boundary integral. The method can be shown to be intrinsically stable for a very large class of time discretizations. When handling discontinuous solutions, an additional stabilization is needed. Often, a nonlinear limiter is introduced, in order to mimic the nonoscillatory behavior of the exact solution, in the spirit of the total variation diminishing (TVD) schemes by Harten [2]. The net effect of this is that in most cases the formal accuracy of the scheme is destroyed not only around the discontinuities of the solution, which is not a surprise, but also around the extrema of the solution, which is more annoying. Moreover, the width of the discontinuities is also affected by the limiter. Of course, this picture can be improved [3,4], but the optimal choice of limiters is by far not known.

On the other hand, another class of schemes exists, the so-called residual distribution (RD) schemes, see [5] for a state of the art. These schemes bear many similarities with the stabilized finite element schemes such as the SUPG scheme [6,7], but the shock capturing method is completely different. It is inspired by the MUSCL [8] and TVD type of schemes.

In this paper, we reformulate the DG schemes so that they can be seen as RD schemes, and this enables us to propose a new class of nonlinear stabilization that does not destroy the formal accuracy of the schemes. This opens an avenue toward nonlinear schemes with *h*-*p* refinement capabilities having a parameter-free nonoscillatory behavior.

The paper is organized as follows. First we recall the standard DG schemes, then show how the RD technique can be introduced. In order to improve the stability, a blending between this RD-DG scheme and the standard DG scheme is introduced. This is possible thanks to the RD formulation of the standard DG scheme. Then numerical results are presented and a conclusion follows. In this paper, we illustrate the technique by a second order accurate scheme for two dimensional scalar equations, the more general case will be considered elsewhere.

Throughout the paper, we consider a triangulation $\mathcal{T}$ with triangular elements. A triangulation is denoted by $\{T_l\}_{l=1,n_t}$. We denote the vertices by $\{M_i\}_{i=1,n_s}$. The approximation space is the space of discontinuous piecewise linear polynomials, $V^h = \bigoplus_{i=1}^{n_t} \mathbb{P}^1(T_i)$, where h is the typical mesh length and $\mathbb{P}^1(T_i)$ is the set of polynomials of degree at most one defined on T_i.

2 Choice of the basis functions

Consider for now a single triangle T. There are several natural bases that generate $\mathbb{P}^1(T)$. If $\{M_j\}_{j=1,3}$ denotes the set of vertices of T, the most natural one is the set of barycentric coordinates denoted by $\{\Lambda_{M_j}\}_{j=1,3}$. They verify $\Lambda_{M_j}(M_k) = \delta_j^k$. The main problem of this basis is that (i) since the elements of V^h are not continuous, it is not that natural to use the

vertices of $\mathcal{T}$ as degrees of freedom; (ii) these basis functions are not L^2-orthogonal. A classical choice in the DG literature is the orthogonal Dubiner basis [9], but polynomials in the Dubiner basis are not associated to any particular physical degree of freedom.

It is possible to construct a set of three polynomials of degree one, with the property that there exist 3 vertices a_1, a_2, a_3 in T, such that the Lagrange interpolants associated to them, denoted by φ_1, φ_2 and φ_3, are orthogonal, i.e.,

$$\int_T \varphi_i(x)\varphi_j(x)dx = \delta_i^j \int_T \varphi_i^2(x)dx.$$

Denoting by

$$\omega_i = \frac{\int_T \varphi_i^2(x)dx}{|T|},$$

we have the quadrature formula

$$\int_T f(x)dx \cong |T| \left(\sum_{j=1}^{3} \omega_j f(a_j) \right). \tag{2.1}$$

This quadrature formula is second order accurate.

An easy calculation indicates that the points a_j are the midpoints of $[G, M_j]$ where G is the centroid of T. By symmetry, $\omega_j = \frac{1}{3}$.

3 Construction of the scheme

The main idea of the paper is to write two schemes for problem (1.1). One is the classical unstabilized DG formulation with the choice of basis functions described in the previous paragraph. Then we show how to rewrite this DG scheme in a Residual Distribution framework, i.e., we define sub-residuals and a total fluctuation. For this, we also introduce another tessellation of the computational domain to which the residuals are naturally associated. The next step is to define a first order monotone scheme that is constructed using this new tessellation and the total residual that is associated to it. Then, using a standard trick in RD schemes, we show how to construct a RD scheme with discontinuous elements. This scheme is non oscillatory and L^∞ stable but not dissipative enough. Hence the last step is to blend the DG and the RD schemes to get a scheme that is essentially non oscillatory, dissipative and formally second order accurate even at extrema.

3.1 DG formulation

Using the weak form of (1.1), we get, for any $\varphi \in \mathbb{P}^1(T)$,

$$\int_T \varphi(x)\frac{\partial u}{\partial t}dx - \int_T \nabla\varphi \cdot \mathbf{f}(u)dx + \int_{\partial T} \varphi(x)\mathbf{f}(u)\cdot\vec{n}d\sigma = 0. \tag{3.1}$$

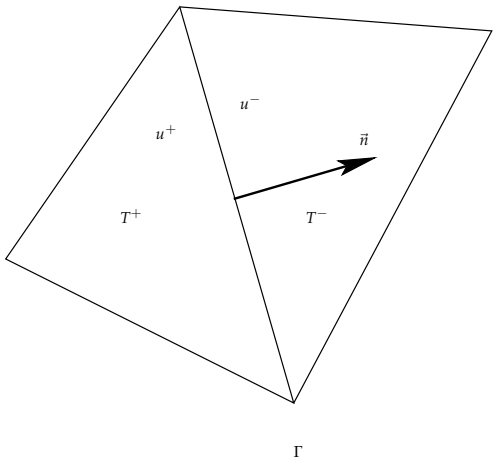

Figure 1: Geometrical parameters.

Using the DG method, and considering $\mathcal{F}(u^+,u^-,\vec{n})$ a numerical flux which is consistent with $\mathbf{f}(u)\cdot\vec{n}$, we get

$$\int_T \varphi(x)\frac{\partial u}{\partial t}dx - \int_T \nabla\varphi\cdot\mathbf{f}(u)dx + \int_{\partial T}\varphi(x)\mathcal{F}(u^+,u^-,\vec{n})d\sigma = 0, \tag{3.2}$$

where u^+ and u^- are the left/right limits of u when the argument in u reaches ∂T. Here, the integral over ∂T is a sum over three edges. For any edge, see Fig. 1, $T^+ = T$ and T^- is the element on the other side of Γ, the vector $\vec{n}$ is the unit vector normal to the edge $T^+\cap T^-$ in the direction $T^+\to T^-$. Accordingly, $u^+ = u_{|T}$ and $u^- = u_{|T^-}$. We choose $\varphi = \varphi_i$ and get

$$|T|\omega_i\frac{du}{dt}(a_i) - \int_T \nabla\varphi_i\cdot\mathbf{f}(u)dx + \int_{\partial T}\varphi_i(x)\mathcal{F}(u^+,u^-,\vec{n})d\sigma = 0. \tag{3.3}$$

Eq. (3.3) can be rewritten in a RD fashion as

$$|T|\omega_i\frac{du}{dt}(a_i) + \Psi_i^{1,T} + \Psi_i^{2,T} + \Psi_i^{3,T} = 0, \tag{3.4}$$

where

$$\Psi_i^{\ell,T} = -\int_{T_\ell}\nabla\varphi_i\cdot\mathbf{f}(u)dx + \int_{\partial T_\ell}\varphi_i(x)\mathcal{F}(u^+,u^-,\vec{n})d\sigma.$$

In this relation, the triangle T has been decomposed into 3 smaller triangles denoted by T_1, T_2, T_3 where the sub-triangle T_ℓ is associated with the edge Γ_ℓ as shown in Fig. 2.

In (3.4) the solution u is replaced by $u^h\in\mathbb{P}^1(T)$, so that we look for a solution of (3.4) in V^h. For the sake of simplicity, we drop the superscript h in u^h but now u belongs to V^h.

The new tessellation we introduce here consists of considering for each edge of the original triangulation the diamond cell associated to it, shown in Fig. 2 as the shaded region.

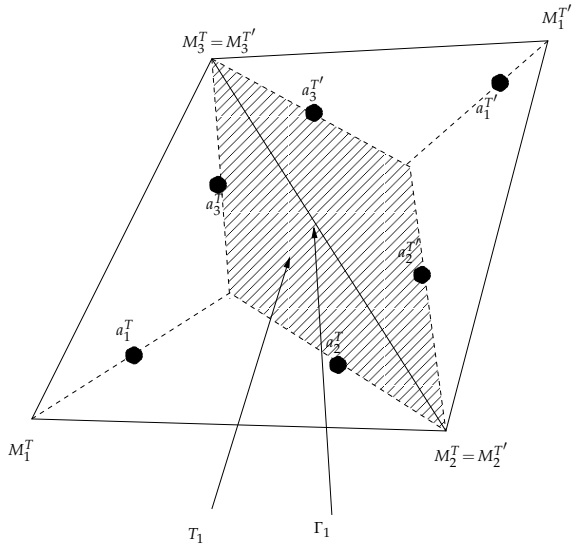

Figure 2: Localization of the Lagrange points. For the triangle T, we have indicated the edge Γ_1 and the sub-triangle T_1. The tessellation element associated to the edge Γ_1 is represented as the shaded region.

The "DG" residuals $\Psi_i^{\ell,T}$ are associated to the edges Γ_ℓ. We have

$$\sum_{a_i^T} \Psi_i^{\ell,T} = \int_{\partial T_\ell} \mathcal{F}(u^+, u^-, \vec{n}) d\sigma$$

because $\sum_{a_i^T} \varphi_i = 1$. Then, if one considers the opposite small triangle T'_ℓ sharing the edge Γ_ℓ with T_ℓ (see Fig. 2), we have, again using the consistency of the numerical flux $\mathcal{F}$,

$$\sum_{a_i^T} \Psi_i^{\ell,T} + \sum_{a_i^{T'}} \Psi_i^{\ell,T'} = \int_{\partial\left(T_\ell \cup T'_\ell\right)} \mathbf{f}(u)\cdot\vec{n} d\sigma,$$

which has the right scaling $\mathcal{O}(h^3)$ for a steady smooth solution (see [10] and Section 3.5). We have one such sub-residual associated with each edge in the triangulation $\mathcal{T}$.

3.2 Residual distribution formulation

Now we look at the same problem seen from a different angle. We define, for any edge Γ_ℓ, a set of monotone residuals that sum up to

$$\Phi_{\Gamma_\ell} := \int_{\partial\left(T_\ell \cup T'_\ell\right)} \mathbf{f}(u)\cdot\vec{n} d\sigma.$$

An example is the following adaptation of the Lax-Friedrichs residual: take $b_i \in \{a_i^T, a_i^{T'}\}_{i=1,\cdot 3}$ and define

$$\Phi_{b_i}^{\Gamma_\ell} = \frac{1}{6}\left(\Phi_{\Gamma_\ell} + \alpha \sum_{b_j \neq b_i} (u(b_i) - u(b_j))\right)$$

for α large enough this is the residual from a monotone RD scheme.

Clearly, we have

$$\sum_{b_i \in \{a_i^T, a_i^{T'}\}_{i=1,\cdot 3}} \Phi_{b_i}^{\Gamma_\ell} = \Phi_{\Gamma_\ell}. \tag{3.5}$$

This relation is the key remark of this paper because it enables us to use the same technique as for RD schemes with continuous elements. In [5, 11] it is explained how, from a first order monotone scheme that satisfies (3.5), to stabilize a higher order RD scheme without destroying its formal accuracy, provided that $\Phi_{\Gamma_\ell} = \mathcal{O}(h^3)$ when u (the interpolant of the exact solution of (1.2)) is smooth.

The next step is to construct a high order monotonicity preserving scheme. Define, for $a \in \mathbb{R}$, $a^+ = \max(a,0)$ and $a^- = \min(a,0)$. We consider

$$x_{b_i}^{\Gamma_\ell} = \frac{\Phi_{b_i}^{\Gamma_\ell}}{\Phi_{\Gamma_\ell}}.$$

Because of (3.5), we have $\sum_{b_i} x_{b_i}^{\Gamma_\ell} = 1$. Notice that

$$\sum_{b_i} (x_{b_i}^{\Gamma_\ell})^+ = 1 - \sum_{b_i} (x_{b_i}^{\Gamma_\ell})^- \geq 1,$$

hence we can define

$$\beta_{b_i}^{\Gamma_\ell} = \frac{(x_{b_i}^{\Gamma_\ell})^+}{\sum_{b_j} (x_{b_j}^{\Gamma_\ell})^+}. \tag{3.6}$$

We now denote

$$\left(\Phi_{b_i}^{\Gamma_\ell}\right)^\star = \beta_{b_i}^{\Gamma_\ell} \Phi_{\Gamma_\ell}, \tag{3.7}$$

and write the limited RD scheme as

$$|T| \omega_i \frac{du}{dt}(a_i) + \sum_{\Gamma_\ell \text{ edge of } T} \left(\Phi_{a_i}^{\Gamma_\ell}\right)^\star = 0. \tag{3.8}$$

For the steady problem (1.2), the resulting scheme, for the degree of freedom $a_i \in T$ is

$$\sum_{\Gamma_\ell \text{ edge of } T} \left(\Phi_{a_i}^{\Gamma_\ell}\right)^\star = 0 \tag{3.9}$$

and this is formally second order accurate.

The schemes (3.7)-(3.8) for problem (1.1), and (3.7)-(3.9) are very different from the DG formulation (3.4).

3.3 Blended scheme

Now we specialize to the steady case (1.2), since the time discretization is more involved for RD schemes than for the DG one: a simple Runge Kutta procedure, whatever its formal accuracy, will not improve the time accuracy for the RD scheme. Indeed, in the RD scheme, space and time have to be coupled because this is a genuinely multidimensional method, see for example [5,12] for some solutions. We will consider the unsteady case in the future.

As for standard residual distribution schemes on conforming meshes, the schemes (3.7)-(3.9) may suffer from iterative convergence problems. Hence, we modify $\left(\Phi_{a_i}^{\Gamma_\ell}\right)^\star$ in (3.7) as

$$\left(\Phi_{a_i}^{\Gamma_\ell}\right)^{\star\star} = \ell\left(\Phi_{a_i}^{\Gamma_\ell}\right)^\star + (1-\ell)\left(\Phi_{a_i}^{\Gamma_\ell}\right)^{\mathrm{DG}}. \tag{3.10}$$

The choice of (3.10) is motivated by the conservation relation (3.5) that is satisfied by both the RD scheme and the DG scheme. This guarantees that if the new scheme is stable, then the numerical solution converges to a weak solution of (1.1): this is shown in Section 3.4. Moreover, if one evaluates (3.10) for the interpolant of a smooth solution of the steady problem (1.2), since both $\left(\Phi_{a_i}^{\Gamma_\ell}\right)^\star$ and $\left(\Phi_{a_i}^{\Gamma_\ell}\right)^{\mathrm{DG}}$ are $\mathcal{O}(h^3)$ in that case, we see that if ℓ is bounded, then $\left(\Phi_{a_i}^{\Gamma_\ell}\right)^{\star\star} = \mathcal{O}(h^3)$. These relations are shown in Section 3.5. Hence the choice of ℓ does not affect the formal accuracy of the blended scheme provided ℓ stays bounded. We choose $\ell \in [0,1]$. The next step is to guarantee the L^∞ stability of the scheme. By construction, the original RD scheme is L^∞ stable, but the DG one is not. The role of the blending parameter is to shut down the DG scheme around discontinuities and to keep it in smooth regions: $\ell \simeq 0$ near discontinuities and $\ell \simeq 1$ in smooth regions.

In the simulations, we have made three choices for ℓ:

- $\ell = 1$ no blending,
- $\ell = 0$ pure DG,
- blended scheme

$$\ell = \frac{\left|\left(\overline{u}_+^k\right)^n - \left(\overline{u}_-^k\right)^n\right|}{\left|\left(\overline{u}_+^k\right)^n\right| + \left|\left(\overline{u}_-^k\right)^n\right|}$$

  with $n=10$. The results are insensitive to the choice of n, provided it is large enough ($n \geq 5$).

The scheme is then (3.9) with (3.7) replaced by (3.10). This is solved by an explicit forward Euler scheme.

3.4 A form of Lax-Wendroff theorem

In this section and the next one, we use again the notation u_h to represent the numerical approximation in order to avoid ambiguities.

The natural question is to see whether or not the schemes of the form (3.8), or more precisely

$$|T|\omega_i\frac{(u_h(a_i)^{n+1}-u_h(a_i)^n)}{\Delta t}+\sum_{\Gamma_\ell \text{ edge of } T}\Phi_{a_i}^{\Gamma_\ell}(u_h^n)=0 \tag{3.11}$$

with the initial conditions $u_h(a_i)^0=u_0(a_i)$ and that satisfies the conservation relation (3.5) can converge to a weak solution of (1.1). The DG scheme, the RD scheme and the blended scheme are, by construction, of this type.

From the knowledge of the family $u_h(a_i)_{a_i\in\mathcal{T}_h}$, one can define an interpolant in V^h. We have the following result

Theorem 3.1. *Let us consider problem* (1.1) *and a family of uniform triangulations $\mathcal{T}_h$ where $h\to 0$. Let us consider the scheme* (3.11) *where the residual satisfies, for any edge Γ_ℓ, the conservation relation* (3.5). *We denote by T_ℓ and T'_ℓ the two triangles that share the edge Γ_ℓ.*

We also assume that the residuals $\Phi_{a_i}^{\Gamma_\ell}$ satisfy the following inequality

$$\left|\Phi_{a_i}^{\Gamma_\ell}\right|\le Ch\sum_{b_j\in T_\ell\cup T'_\ell}\left|u_h(a_i)-u_h(b_j)\right|.$$

If the sequence u_h is uniformly bounded by a constant $C(u_0)$ independent of h and if a subsequence converges in $L^2(\mathbb{R}^2)$ to a $L^2\cap L^\infty$ function u, then u is a weak solution of (1.1).

Proof. Let $t_f>0$ and φ a compactly supported test function of $\mathbb{R}^2\times[0,t_f$. If one multiplies (3.11) by $\varphi(a_i,t_n)$, we have, denoting by $|T|$ the area of T,

$$\sum_{n=0}^{N}\Delta t\sum_{a_i}\varphi(a_i,t_n)\left(|T|\omega_i\frac{(u_h(a_i)^{n+1}-u_h(a_i)^n)}{\Delta t}+\sum_{\Gamma_\ell \text{ edge of } T}\Phi_{a_i}^{\Gamma_\ell}(u_h^n)\right)=0.$$

Then we re-arrange the first term and we get

$$\begin{aligned}&\sum_{n=0}^{N}\Delta t\sum_{a_i}\varphi(a_i,t_n)|T|\omega_i\frac{(u_h(a_i)^{n+1}-u_h(a_i)^n)}{\Delta t}\\&=-\sum_{n=1}^{N}\sum_{a_i}|T|\omega_i\Delta t\frac{\varphi(a_i,t_n)-\varphi(a_i,t_{n-1})}{\Delta t}u_h(a_i)^n-\sum_{a_i}\omega_i|T|\,\varphi(a_i,t_0)u_0(a_i),\end{aligned}$$

and a classical argument shows that the right hand side converges, under the assumptions we have made, to

$$-\int_{\mathbb{R}^2\times\mathbb{R}^+}\frac{\partial\varphi}{\partial t}u(x,t)dxdt-\int_{\mathbb{R}^2}\varphi(x,t)u_0(x)dx.$$

We now consider the second term. For any edge Γ_ℓ, we denote by T^+ and T^- the two triangles that share that edge Γ_ℓ and as in Section 3.1, we have the subtriangles T_ℓ^+ and

T_ℓ^- attached to the edge Γ_ℓ as T_1 for Γ_1 in Fig. 2. We introduce the DG residuals

$$\Psi_i^{\ell,T^+} = -\int_{T_\ell^+} \nabla\varphi_i\cdot\mathbf{f}(u_h)dx + \int_{\partial T_\ell^+} \varphi_i(x)\mathcal{F}(u_h^+,u_h^-,\vec{n})d\sigma,$$
$$\Psi_i^{\ell,T^-} = -\int_{T_\ell^-} \nabla\varphi_i\cdot\mathbf{f}(u_h)dx + \int_{\partial T_\ell^-} \varphi_i(x)\mathcal{F}(u_h^+,u_h^-,\vec{n})d\sigma;$$

and write

$$\sum_{n=0}^{N}\Delta t\sum_{a_i}\varphi(a_i,t_n)\sum_{\Gamma_\ell \text{ edge of } T}\Phi_{a_i}^{\Gamma_\ell}(u_h^n)$$
$$=\sum_{n=0}^{N}\Delta t\sum_{\text{edges}}\sum_{T=T^+,T^-}\sum_{a_i\in T}\varphi(a_i,t_n)\Psi_i^{\ell,T}+\sum_{n=0}^{N}\Delta t\sum_{\text{edges}}\sum_{a_i\in T^+\cup T^-}\varphi(a_i,t_n)\big(\Phi_{a_i}^{\Gamma_\ell}(u_h^n)-\Psi_i^{\ell,T}\big).$$

First, since φ is compactly supported and using the consistency of the numerical flux $\mathcal{F}$, we have

$$\sum_{\text{edges}}\sum_{T=T^+,T^-}\sum_{a_i\in T}\varphi(a_i,t_n)\Psi_i^{\ell,T} = -\int_{\mathbb{R}^2}\nabla\varphi(x,t_n)\cdot\mathbf{f}(u_h(x,t_n))dx,$$

so that using again the boundedness of u_h, and classical arguments (see [13]), we have

$$\sum_{n=0}^{N}\Delta t\sum_{\text{edges}}\sum_{T=T^+,T^-}\sum_{a_i\in T}\varphi(a_i,t_n)\Psi_i^{\ell,T}\to -\int_{\mathbb{R}^2\times\mathbb{R}^+}\nabla\varphi(x,t)\cdot\mathbf{f}(u(x,t))dxdt.$$

Using the conservation relation, we have

$$\sum_{a_i\in T^+\cup T^-}\varphi(a_i,t_n)\big(\Phi_{a_i}^{\Gamma_\ell}(u_h^n)-\Psi_i^{\ell,T}\big)=\sum_{a_i\in T^+\cup T^-}(\varphi(a_i,t_n)-\varphi(a_{i_0},t_n)\big(\Phi_{a_i}^{\Gamma_\ell}(u_h^n)-\Psi_i^{\ell,T}\big),$$

where a_{i_0} is any of the element of $T^+\cup T^-$.

Using the consistency of the numerical flux, the second term is bounded by

$$\Psi_i^{\ell,T} = -\int_{T_\ell}\nabla\varphi_i\cdot\mathbf{f}(u_h)dx+\int_{\partial T_\ell}\varphi_i(x)\mathcal{F}(u_h^+,u_h^-,\vec{n})d\sigma$$
$$=-\int_{T_\ell}\nabla\varphi_i\cdot\big(\mathbf{f}(u_h)-\mathbf{f}(u_h(a_{i_0}))\big)dx+\int_{\partial T_\ell}\varphi_i(x)\big(\mathcal{F}(u_h^+,u_h^-,\vec{n})-\mathcal{F}(u_h(a_{i_0}),u_h(a_{i_0}),\vec{n})\big)d\sigma$$

and we get

$$\big|\Psi_i^{\ell,T}\big|\le Ch\sum_{b_j\in T^+\cup T^-}\big|u_h(a_i)-u_h(b_j)\big|.$$

This shows that $\Phi_{a_i}^{\Gamma_\ell}(u_h^n)-\Psi_i^{\ell,T}$ satisfies a similar inequality and we get

$$\Big|\sum_{a_i\in T^+\cup T^-}\varphi(a_i,t_n)\big(\Phi_{a_i}^{\Gamma_\ell}(u_h^n)-\Psi_i^{\ell,T}\big)\Big|\le C\big|\big|\nabla\varphi\big|\big|_\infty h^2\sum_{b_i,b_j\in T^+\cup T^-}\big|u_h(b_i)-u_h(b_j)\big|.$$

Since the triangulation is uniform, we conclude by using the lemma 3.1 whose proof can be found in [11] or [14]. □

Lemma 3.1. Let $\mathcal{Q}$ be a compact set of $\mathbb{R}^2$. Under the assumptions of theorem 3.1, we have

$$\lim_h \left(\sum_{n=0}^{N} \Delta t \sum_{\text{edges} \subset \mathcal{Q}} |T_\ell^+ \cup T_\ell^-| \sum_{a_i, a_j \in T_\ell^+ \cup T_\ell^-} \left| u(a_i) - u(a_j) \right| \right) = 0.$$

Here, $|T_\ell^+ \cup T_\ell^-|$ is the measure of $T_\ell^+ \cup T_\ell^-$

3.5 Accuracy considerations.

In this paragraph, we show that if we have a scheme

$$\sum_{\Gamma_\ell \text{ edge of } T} \Phi_{a_i}^{\Gamma_\ell} = 0, \tag{3.12}$$

where the residuals satisfy the conservation relation (3.5) and are of the form (3.7)

$$\Phi_{a_i}^{\Gamma_\ell} = \beta_{a_i}^{\Gamma_\ell} \Phi_{\Gamma_\ell},$$

then the scheme is (formally) second order accurate for the *steady* problem (1.2).

To show this, we start from the same algebraic considerations as in the previous section, but specialized to steady problems. We have (using the same notations)

$$\int_{\mathbb{R}^2} \nabla \varphi(x) \mathbf{f}(u_h(x)) dx + \sum_{\text{edges}} \sum_{a_i \in T^+ \cup T^-} (\varphi(a_i) - \varphi(a_{i_0})) \left(\Phi_{a_i}^{\Gamma_\ell}(u_h) - \Psi_i^{\ell,T} \right) = 0. \tag{3.13}$$

Assuming that the solution of (1.2) is smooth, we have

$$\int_{\mathbb{R}^2} \nabla \varphi(x) \mathbf{f}(u(x)) dx = 0$$

and for any triangle T

$$\int_T \nabla \mathbf{f}(u(x)) dx = 0, \quad \Psi_i^{\ell,T}(u) = 0.$$

The last relation comes from the very definition of the DG scheme (3.3), so that using the form of the residual,

$$\underbrace{\int_{\mathbb{R}^2} \nabla \varphi(x) \left(\mathbf{f}(u_h(x)) - \mathbf{f}(u(x)) \right) dx}_{\text{I}}$$

$$+ \sum_{\text{edges}} \sum_{a_i \in T^+ \cup T^-} (\varphi(a_i) - \varphi(a_{i_0})) \times \left(\beta_{a_i}^{\Gamma_\ell} \left(\underbrace{\Phi_{\Gamma_\ell}(u_h) - \Phi_{\Gamma_\ell}(u)}_{\text{II}} \right) - \left(\underbrace{\Psi_i^{\ell,T}(u_h) - \Psi_i^{\ell,T}(u)}_{\text{III}} \right) \right) = 0.$$

Using standard interpolation techniques and the smoothness of the flux $\mathbf{f}$, we can see that the term I is $\mathcal{O}(h^2)$. Similarly, using the same arguments as in [11], we see that

$$\Psi_i^{\ell,T}(u_h) - \Psi_i^{\ell,T}(u) = \mathcal{O}(h^3),$$
$$\Phi_{\Gamma_\ell}(u_h) - \Phi_{\Gamma_\ell}(u) = \mathcal{O}(h^3),$$

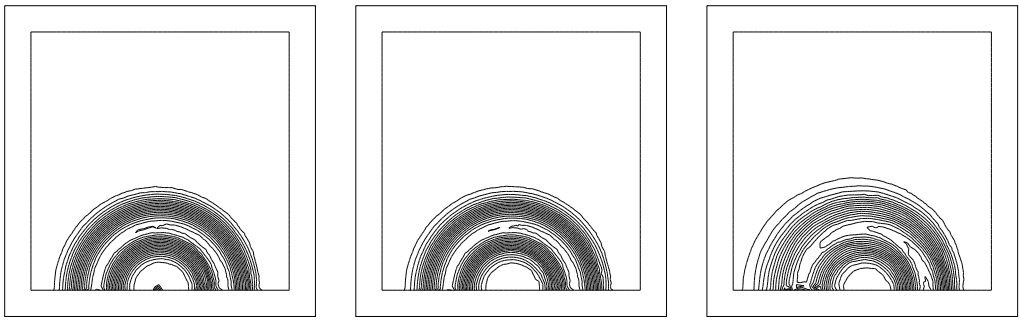

DG Blend ($n=10$) scheme (3.9)

Figure 3: Solutions for (4.1).

so that, assuming that the mesh is regular, we have the truncation error

$$\sum_{\Gamma_\ell \text{ edge of } T} \Phi_{a_i}^{\Gamma_\ell}(u) = \mathcal{O}(h^2). \tag{3.14}$$

Proposition 3.1. Assume that the mesh is regular. If the solution of (1.2) is smooth and if the conservation relation (3.5) holds, the scheme (3.12), where $\Phi_{a_i}^{\Gamma_\ell}$ is defined by (3.7), has the truncation error (3.14).

Remark 3.1. The proof of Proposition 3.1 indicates why it is important that the PDE be a steady one. In case of an unsteady problem, standard Runge Kutta methods cannot work because there is an inconsistency between the space and time integration In the present technique, they *must* be coupled. This can be achieved nevertheless, either by space-time methods or by "pre-discretizing" the $\partial/\partial t$ term as in finite element methods. See [12] for some examples.

4 Numerical results

We have tested the scheme on two examples, a convection problem and the Burgers equation.

4.1 Convection problem

The problem is to solve

$$\begin{aligned} &-x\frac{\partial u}{\partial y}+y\frac{\partial u}{\partial x}=0, \quad (x,y)\in[0,1]\times[0,1], \\ &u(x,0)=\begin{cases} -\sin\left(\pi(2x-0.2)/0.6\right) & \text{if } 0.1\le x\le 0.4, \\ 0 & \text{else.} \end{cases} \end{aligned} \tag{4.1}$$

The solutions obtained by the different schemes are displayed in Fig. 3. A cross-section (at $x=0$) is displayed in Fig. 4. We see that the results obtained for the DG and blended

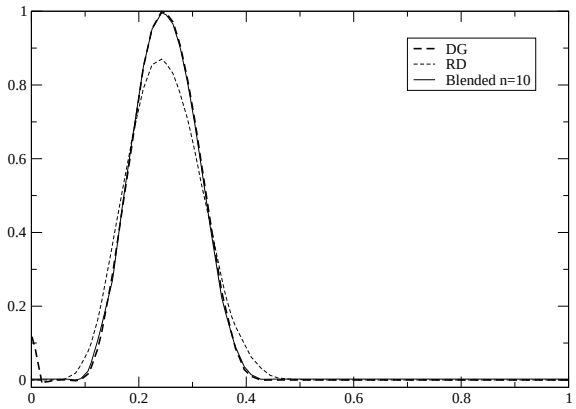

Figure 4: Cross-section of the solutions at $x=0$.

schemes are much more accurate than that of the RD scheme, and the blended one is nonoscillatory.

We have done an error analysis in the L^∞ and L^1 norms. The results, given in Table 1, indicate that the blended scheme is second order accurate while the original residual distribution scheme is only first order accurate because the iterative scheme is not convergent, as expected.

Table 1: Error analysis for the convection problem.

h	L^∞	order (L^∞)	L^1	order (L^1)
1.57e-2	2.33e-2	–	5.55e-3	–
7.86e-3	8.89e-3	1.39	6.80e-4	1.52
7.86e-4	6.89e-4	1.11	6.77e-7	1.50
1.57e-4	1.35e-4	1.01	5.42e-9	1.50
7.86e-5	6.76e-5	1.00	6.77e-10	1.50
Results for the RD scheme				
1.57e-2	1.90e-3	–	2.26e-4	–
7.86e-3	4.16e-4	2.20	1.52e-5	1.95
1.57e-3	6.64e-6	2.57	2.21e-8	2.03
7.86e-4	1.66e-6	2.00	1.38e-9	2.00
7.86e-5	1.66e-8	2.00	1.38e-13	2.00
Results for the blended scheme				
1.57e-2	6.64e-4	–	2.21e-4	–
7.86e-3	1.60e-4	2.06	1.38e-5	2.00
1.57e-3	6.64e-6	1.98	2.21e-8	2.00
7.86e-4	1.66e-6	2.00	1.38e-9	2.00
7.86e-5	1.66e-8	2.00	1.38e-13	2.00
Results for the DG scheme				

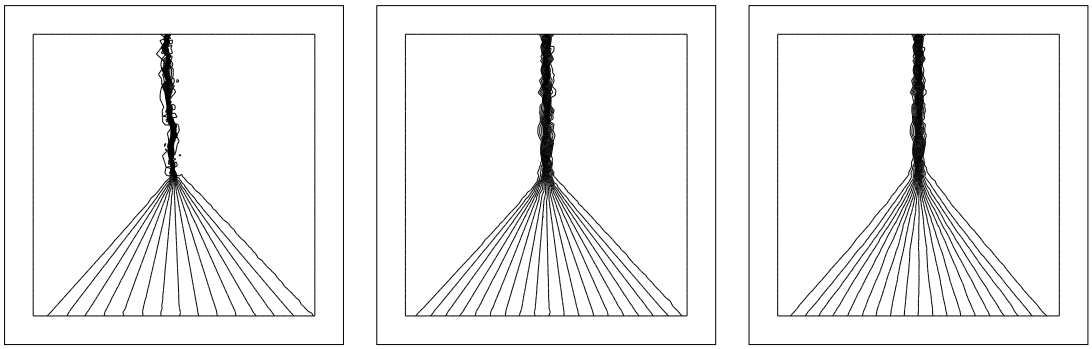

DG Blend ($n=10$) scheme (3.9)

Figure 5: Solutions for (4.2).

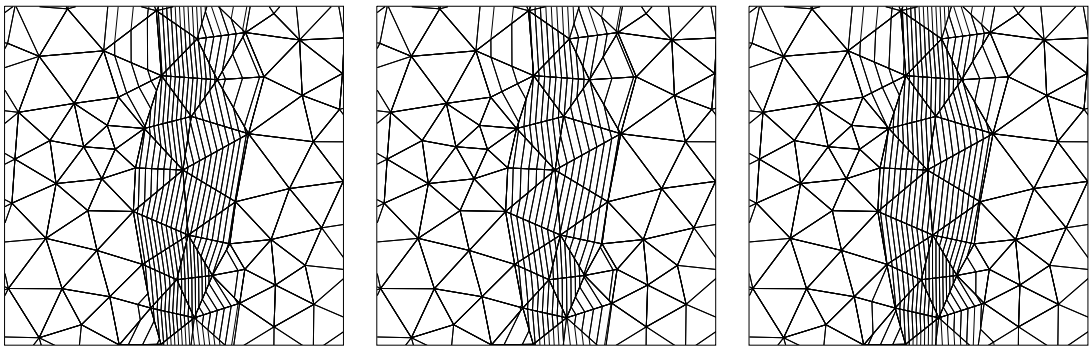

DG Blend scheme (3.9)

Figure 6: Zoom-in pictures for (4.2).

4.2 Burgers problem

Here, we are solving

$$\begin{aligned} &\frac{1}{2}\frac{\partial u^2}{\partial x}+\frac{\partial u}{\partial y}=0, \quad (x,y)\in]0,1[^2, \\ &u(x,y)=\begin{cases} 1-2x & x\in[0,1],\ y=0, \\ 1.5 & x=0,\ y\in[0,1], \\ 0.5 & x=1,\ y\in[0,1]. \end{cases} \end{aligned} \tag{4.2}$$

The solutions are displayed in Fig. 5 with zoomed pictures to show the width of the shock structure shown in Fig. 6.

We also show cuts in the fan, see Fig. 7 where the oscillation-free nature of the RD and blended schemes can be seen. A close inspection of the same figure shows that the DG and blended solutions are indistinguishable in the fan ($y=0.1$).

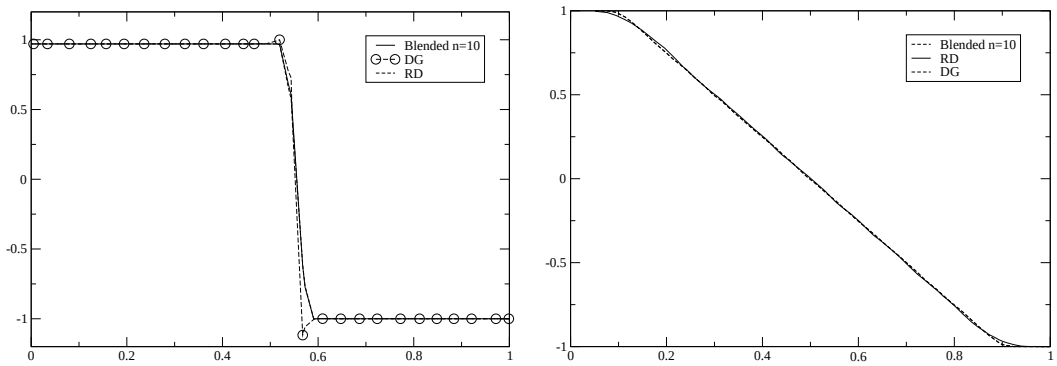

Figure 7: Cuts across the shock and the fan.

5 Conclusions

In this paper, we have presented results on a new scheme that is able to combine the advantages of the DG schemes (compact stencil, *h-p* refinement capabilities, accuracy) and those of the RD schemes (compact stencil, accuracy, parameter-free oscillation control around discontinuities). The results are presented for a formally second order scheme, however there is no problem in principle to extend the approach to more than second order accuracy, as well as to unsteady problems following [12,15,16]. We have also given examples for conforming meshes, but the method can easily be extended to non conforming ones just by introducing hanging nodes.

In the future we wish to elaborate on this method by showing how genuinely very high order parameter-free schemes can be constructed having this residual property on possibly non conforming meshes. Another research topic is to simplify our method, i.e., to avoid computing *two* schemes to reach accuracy and stability.

Acknowledgments

The first author was supported in part by the EU STREP ADIGMA and a CNES grant. This research was conducted in part during the second author's visit in the INRIA project ScAlApplix in May 2006, as an invited professor. The research of the second author was also supported in part by NSF grant DMS-0510345.

References

[1] B. Cockburn and C.-W. Shu. Runge-kutta discontinuous Galerkin methods for convection-dominated problems. *J. Sci. Comput.*, 16:173–261, 2001.

[2] A. Harten. High resolution schemes for hyperbolic conservation laws. *J. Comput. Phys.*, 49:357–393, 1983.

[3] R. Biswas, K. D. Devine, and J.E. Flaherty. Parallel, adaptive finite element methods for conservation laws. *Appl. Numer. Math.*, 14:255–283, 1994.
[4] A. Burbeau. *Méthodes de Galerkine discontinu d'ordre élevé pour la simulation instationnaire en maillage non structuré*. PhD thesis, Ecole doctorale Mathématique et Informatique, Université de Bordeaux I, 2000.
[5] Deconinck H, editor. *34th CFD High Order Discretization Methods*. von Kármán Institute, November 2005.
[6] Th.J.R. Hughes, L.P. Franca, and M. Mallet. Finite element formulation for Computational Fluid Dynamics : I symmetric forms of the compressible Euler and Navier Stokes equations and the secoond law of thermodynamics. *Comput. Methods Appl. Mech. Engrg*, 54:223–234, 1986.
[7] Th.J.R. Hughes and M. Mallet. A new finite element formulation for Computational Fluid Dynamics : IV a discontinuity–capturing operator for multidimensional advective–diffusive systems. *Comput. Methods Appl. Mech. Engrg*, 58:329–336, 1986.
[8] B. van Leer. Towards the ultimate conservative difference scheme ii. monotonicity and conservation combined in a second order scheme. *J. Comput. Phys.*, 14:361–370, 1974.
[9] M. Dubiner. Spectral methods on triangles and other domains. *J. Sci. Comput.*, 6:345–390, 1991.
[10] R. Abgrall. Towards the ultimate conservative scheme: following the Quest. *J. Comput. Phys.*, 167(2):277–315, 2001.
[11] R. Abgrall and P. L. Roe. High-order fluctuation schemes on triangular meshes. *J. Sci. Comput.*, 19(1-3):3–36, 2003.
[12] R. Abgrall, N. Andrianov, and M. Mezine. Towards very high-order accurate schemes for unsteady convection problems on unstructured meshes. *Int. J. Numer. Meth. Fluids*, 47(8-9):679–691, 2005.
[13] E. Godlewski and P.-A. Raviart. *Numerical approximation of hyperbolic systems of conservation laws.* Applied Mathematical Sciences. 118. New York, NY: Springer , 1996.
[14] C.-S. Chou and C.-W. Shu. High order residual distribution conservative finite difference WENO schemes for convection-diffusion steady state problems on non-smooth meshes. *J. Comput. Phys.*, 224(2):992–1020, 2007.
[15] R. Abgrall and M. Mezine. Construction of second order accurate monotone and stable residual distribution schemes for unsteady flow problems. *J. Comput. Phys.*, 188(1):16–55, 2003.
[16] M. Ricchiuto, Á. Csík, and H. Deconinck. Residual distribution for general time dependent conservation laws. *J. Comput. Phys.*, 209(1):249–289, 2005.